QCD studies with ATLAS at the LHC

V. A. Mitsou[a], on behalf of the ATLAS Collaboration

[a]Instituto de Física Corpuscular (IFIC), CSIC - Universitat de València,
Edificio Institutos de Investigación, Apartado de Correos 22085
E-46071 Valencia, Spain

The study of QCD processes at the LHC will serve two main goals. First, the predictions of Quantum Chromodynamics will be tested and precision measurements will be performed, allowing additional constraints to be established, and providing measurements of the strong coupling constant. Second, QCD processes represent a major part of the background to other Standard Model processes and signals of new physics at the LHC and therefore need to be understood in depth. An overview of various measurements of QCD-related processes to be performed at the LHC is presented, based on final states containing high-$p_{\rm T}$ leptons, photons and jets. Moreover, possible deviations from QCD predictions indicating presence of new physics are discussed.

1. INTRODUCTION

The Large Hadron Collider (LHC) is a proton-proton collider with a 14-TeV centre-of-mass energy planned to be operated at a luminosity of 10^{34} cm^{-2}s^{-1}. This luminosity will result in large event samples for most processes such as $\sim 10^8$ leptonic W decays, $\sim 10^4$ photons with $p_{\rm T} > 500$ GeV and $\sim 10^4$ jets with $p_{\rm T} > 1$ TeV. With these data, the theory of strong interactions will be precisely tested and detailed measurements can be performed leading to new information on the parton densities of the proton and possibly to constraints of the strong coupling constant in yet unexplored regions. Figure 1 displays the region in the (x, Q^2) plane which will be covered by LHC in comparison with HERA and fixed-target experiments.

This report presents an overview of QCD studies at the LHC, assuming the expected performance of the ATLAS experiment, which is briefly described in Section 2. First, issues related to minimum-bias events (Section 3) and hard diffractive scattering (Section 4) are presented. Next, the information to be deduced from the measurements of jets (Section 5) is described, followed by a section on photon physics (Section 6) and one concerning the production of Drell-Yan pairs and heavy gauge bosons (Section 7). In Section 8, the production of heavy flavours is discussed. Before concluding, the discovery of new physics, such as quark compositeness, through the observation of deviations from QCD predictions is addressed. More details on QCD studies in ATLAS can be found in Ref. [1].

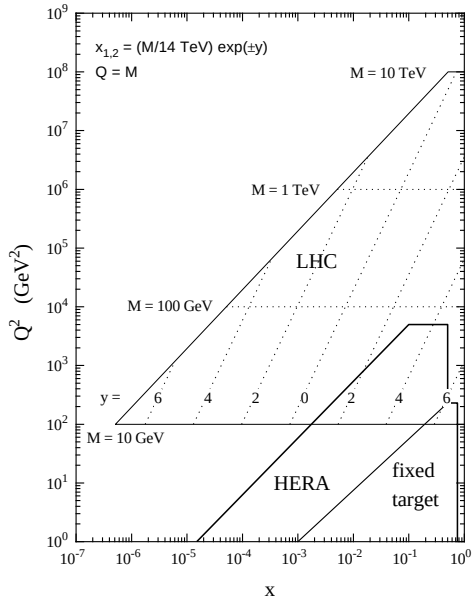

Figure 1. Parton kinematics at the LHC in the (x, Q^2) kinematic plane for the production of a particle of mass M at rapidity y [2].

Table 1
Basic performance characteristics of the ATLAS detector for the LHC.

Detector sub-system	Performance
Tracking (Si + transition radiation detector)	$\sigma/p_{\rm T} \simeq 5 \cdot 10^{-4}\ p_{\rm T}({\rm GeV}) + 1\%$
EM calorimeter (Pb + liquid Ar)	$\sigma/E \simeq 10\%/\sqrt{E({\rm GeV})}$
Hadronic barrel calorimeter (steel + scintillator)	$\sigma/E \simeq 50\%/\sqrt{E({\rm GeV})} + 3\%$
Hadronic end-cap calorimeter (Cu/W + liquid Ar)	$\sigma/E \simeq 60\%/\sqrt{E({\rm GeV})} + 3\%$
Muon spectrometer (air toroidal magnet)	$\sigma/p_{\rm T} \simeq 10\%$ at $p_{\rm T} \sim 1$ TeV

2. THE ATLAS EXPERIMENT

The ATLAS detector [3] is a general-purpose experiment designed to be sensitive to the various physics processes expected to take place at the LHC. The design luminosity of 10^{34} cm^{-2}s^{-1} will allow for high-statistics samples to be collected, resulting in measurements limited in precision mostly by systematic uncertainties. Most of the QCD-related studies will take place during the initial operation at a (low) luminosity of 10^{33} cm^{-2}s^{-1}, delivering a total of 10 fb^{-1} per year.

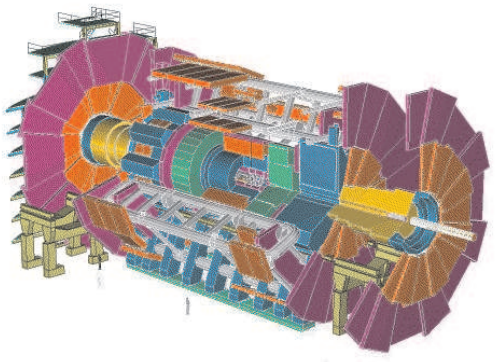

Figure 2. Schematic view of the ATLAS detector.

This hermetic apparatus provides pseudorapidity coverage of up to $|\eta| < 2.5$ for tracking, extended to $|\eta| < 5$ for calorimetry, while muons will be accurately measured up to $|\eta| < 2.7$. It comprises a high-performance tracker consisting of silicon detectors and a transition radiation tracker in a 2-T solenoidal magnetic field, a high-resolution electromagnetic calorimeter based on lead/liquid argon, a hadronic calorimeter combining steel/scintillator and Cu-W/liquid argon, and a large muon spectrometer embedded in an air-core toroidal magnet. The basic performance parameters of these systems are given in Table 1 and a schematic view of the ATLAS detector is shown in Fig. 2.

3. MINIMUM-BIAS INTERACTIONS

Due to the high luminosity at the LHC, there will be up to an average of 25 inelastic collisions per bunch-crossing. In order to understand precisely their contribution to the measured quantities for the hard scattering events of interest, a detailed knowledge of the structure of the minimum-bias events is required.

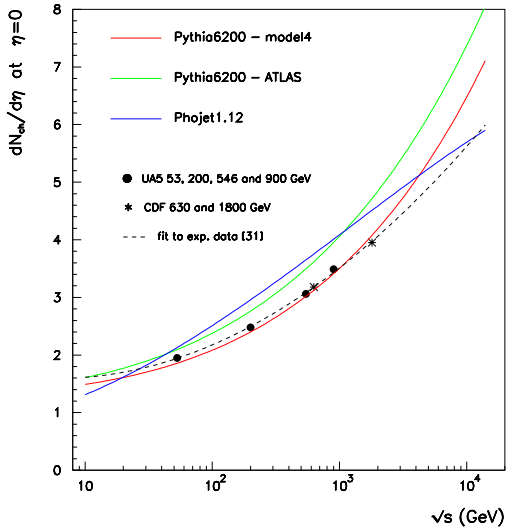

Figure 3. Charged particle density $\mathrm{d}N_{\rm ch}/\mathrm{d}\eta$ at $|\eta| = 0$ as a function of $\sqrt{s}$ [4]. PYTHIA and PHOJET predictions are compared with UA5 and CDF data.

Several studies have been done performing comparisons between various Monte Carlo simulation programs. In particular [4], PYTHIA6.200 [5] and PHOJET1.12 [6] predictions are found to be in good agreement with experimental data for energies below 800 GeV, as far as the inelastic cross section is concerned, however they diverge at the level of $\sim$15% at higher energies. Figure 3 displays the charged particle density $\mathrm{d}N_{\mathrm{ch}}/\mathrm{d}\eta$ at $|\eta| = 0$ as a function of $\sqrt{s}$ per pp collision. The generators predictions are compared with experimental data from UA5 [7] and CDF [8]. PYTHIA6.200 provides a better description for energies up to $\sim$3 TeV, nevertheless the extrapolation of the fit-to-experimental-data to the LHC energy favours PHOJET1.12. More studies are needed to develop accurate theoretical models for minimum-bias events.

4. HARD DIFFRACTIVE PROCESSES

The understanding of diffractive phenomena, i.e. processes that arise from the exchange of colour-neutral objects, has received revived attention in the last few years due to the appearance of hard diffractive process, i.e. diffractive processes in which a hard scatter takes place. They appear either as single (AB $\rightarrow$ AX or AB $\rightarrow$ BX) or double (AB $\rightarrow$ ABX) diffractive processes. Diffractive events are characterized by the occurrence of large rapidity gaps and, in the case of single-diffractive events, by the appearance of a leading hadron, i.e. a hadron with a momentum close to the beam momentum separated from the diffractive final state X.

The advantage of the LHC is in the production of diffractive final states with large masses, allowing the probing of partonic structure with a variety of different processes [9]. A selection of events with two leading protons or rapidity gaps on both sides of the detector transforms the proton-proton collider into a Pomeron-Pomeron collider with variable beam energy, where the maximal centre-of-mass energy ranges between the one of the Sp$\bar{\mathrm{p}}$S and the Tevatron collider.

An extension of the LHC detectors in the very forward region beyond $|\eta| = 5$ (Roman Pot systems more than 100 m away from the interaction point) is planned by the CMS [10] (TOTEM [11] detector) collaboration and is under study by the ATLAS collaboration. It would increase the acceptance for charged particles from inelastic interactions and provide tagging and measurements of leading protons from elastic and diffractive interactions.

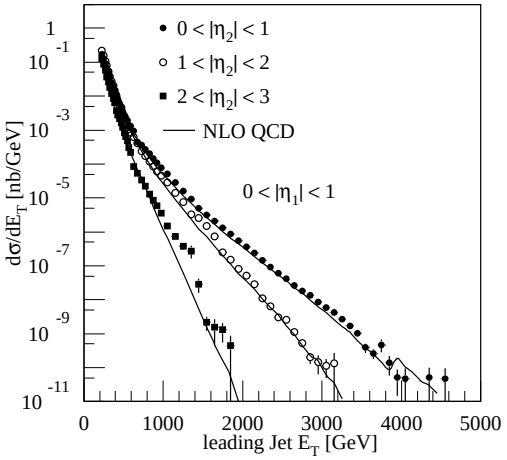

Figure 4. Di-jet cross section at hadron level with a leading jet with $|\eta_1| < 1$ for different ranges of the pseudorapidity of the second leading jet as obtained from PYTHIA (points) and from a NLO Monte Carlo calculation (solid line) [12].

5. JET SIGNATURES

Measurements of jets allow conclusions to be drawn on the hard scattering process taking into account the evolution of the partonic system from the hard scattering to the observed set of hadrons, i.e. the parton showering, the fragmentation, the short-lived particle decays and the multiple interactions [12]. Important systematic uncertainties (the statistical ones are small at the LHC) are, e.g., the jet algorithm, the energy scale (especially at very large E_{T}) and the underlying event.

The expected statistics for inclusive jet production at the LHC for an integrated luminosity of 30 fb^{-1} amounts to $4 \cdot 10^4$ events with $E_{\mathrm{T}}^{\mathrm{jet}} > 1$ TeV, 3000 events with $E_{\mathrm{T}}^{\mathrm{jet}} > 2$ TeV and ~ 40 events with $E_{\mathrm{T}}^{\mathrm{jet}} > 3$ TeV. Figure 4 shows the di-jet differential cross section for different jet rapidities and for a minimal transverse energy of

180 GeV. The measurement of di-jet events and their properties for different values of the minimal $E_{\rm T}$ and of the two jet pseudorapidities can be used to constrain the parton densities inside the proton in various kinematic regions of the (x, Q^2) plane.

A study [13] was carried out by ATLAS to evaluate a method which allows the extraction of the strong coupling constant, α_s, from an inclusive jet cross section measurement based on a parameterization of the α_s dependence. The approach taken is to fit the jet cross section as a function of $E_{\rm T}$ and $\alpha_s(E_{\rm T})$ in two ranges of pseudorapidity and study its sensitivity to different sets of parton distribution function (pdf). By inverting this fit, the determination of $\alpha_s(E_{\rm T})$ is possible. An example of this analysis is shown in Fig. 5, where both the generated and reconstructed values of $\alpha_s(E_{\rm T})$ are plotted. The residual bias in terms of $\alpha_s(E_{\rm T})$ is in average of the order of a few percent. The results indicate that α_s can be determined with an overall precision of $\sim$10%, in which the contribution to the uncertainty from our knowledge of pdf's is $\sim$3%.

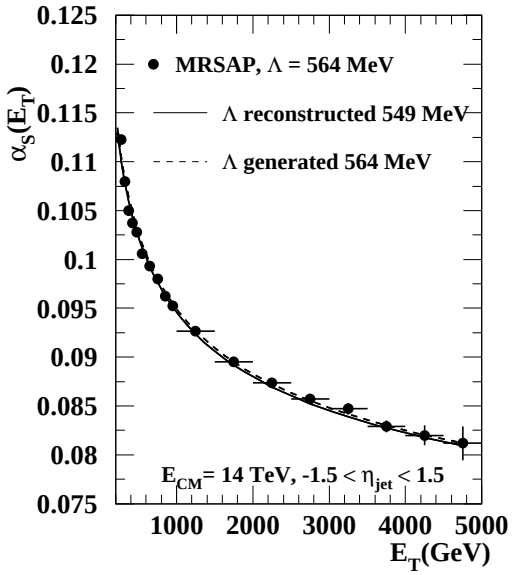

Figure 5. Extracted values of $\alpha_s(E_T)$ (points), fitted with the evolution function to determine $\Lambda^{(4)}_{\overline{\rm MS}}$ (solid line) and the evolution used in the generation of the cross section (dashed line) [13].

6. PHOTON SIGNATURES

Direct photon measurements can provide important constraints on parton distributions, especially on the gluon distribution in the proton. The advantage of photon measurements is the better energy determination in comparison to jet measurements. In the case of photons, however, the experimental background due to jets containing a leading π^0 has to be well understood. Photon identification in ATLAS is based on the shower shapes in the calorimeters, conversion reconstruction and a track veto. However, γ/jet separation power can be enhanced if isolation criteria [14] are applied around the shower, i.e. no significant hadronic activity is allowed in a cone around the photon direction. Figure 6 shows the dependence of the jet rejection on the transverse energy at low luminosity with and without isolation cuts. For an 80% photon efficiency for photons from H $\rightarrow \gamma\gamma$ decays, a jet rejection of 1440 (880) is achieved at low (design) luminosity.

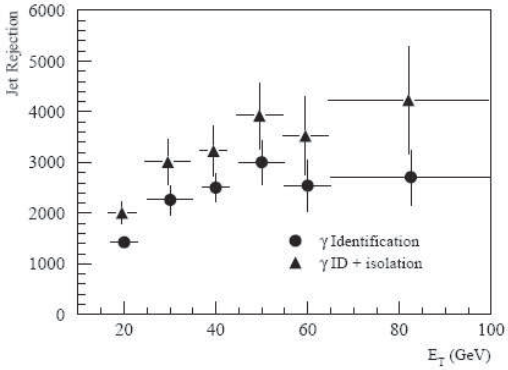

Figure 6. Jet rejection after photon identification and isolation cuts as a function of the jet $E_{\rm T}$ at low luminosity. The tuning was done so as to achieve an 80% efficiency for photons coming from Higgs decays [14].

The direct production of photons can provide sensitivity to the gluon density in the proton via the QCD Compton process, qg $\rightarrow \gamma$q [15]. Figure 7 displays the differential cross section for direct photon production with an opposite-side jet ($150^\circ < \Delta\phi_{\gamma-{\rm jet}} < 210^\circ$) for the LHC energy. The QCD Compton process clearly domi-

nates over the annihilation graph, $q\bar{q} \rightarrow \gamma g$. The CTEQ4L [16] set is used for the parameterization of the proton, while other sets such as CTEQ4HJ, MRS(A) [17] and GRV94HO [18] give similar results within 10%.

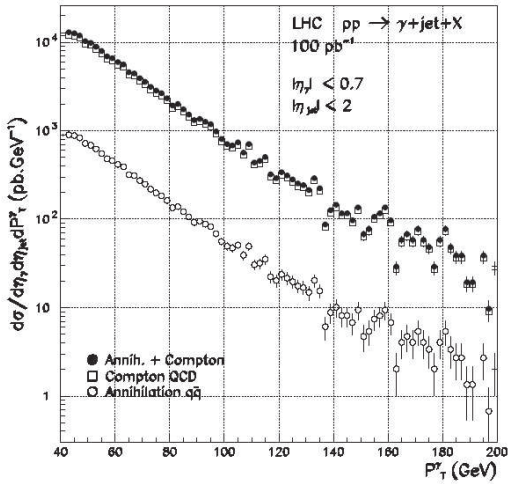

Figure 7. Direct photon production with an opposite-side jet as a function of p_{T}^{γ} obtained from PYTHIA and the CTEQ4L structure function [15].

The method used to extract the gluon structure function, $xG(x)$, is based on fitting the $\gamma-$jet cross section with the theoretical prediction at LO. In this example, the MRS(A) set is used to parameterize the quarks pdf's and the CTEQ set is adopted for $xG(x)$. The results for the gluon density in the proton are shown in Fig. 8 in comparison with UA2 [19] data and the HMRS B1 [20] theoretical prediction, with which they are in good agreement. The gluon density can be determined in the range $0.005 < x < 0.04$ and $440\ \mathrm{GeV}^2 < Q^2 < 2 \cdot 10^4\ \mathrm{GeV}^2$ with a systematic error of 10–20%, which can be reduced if NLO calculation is used for the cross section.

7. LEPTONIC FINAL STATES

The measurement of Drell-Yan lepton pair production and the production of W and Z bosons (with a leptonic decay to electrons or muons) will allow constraints to be set on the quark and anti-

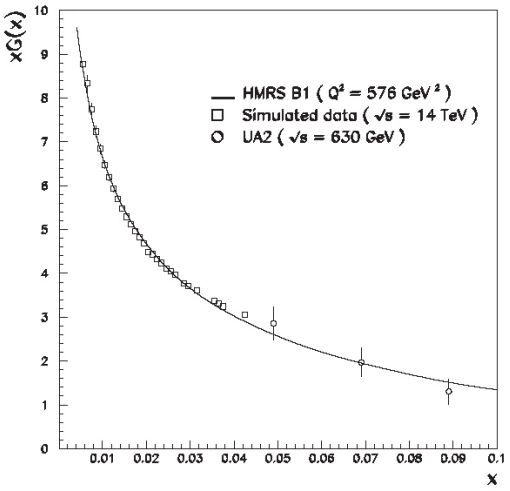

Figure 8. Comparison between theoretical prediction, ATLAS simulated data and data from the UA2 experiment [15].

quark densities of the proton at a scale given by the invariant mass of the lepton pair or by the W/Z boson mass over a wide range in Bjorken x [1]. QCD effects enter the cross section of these processes only in the initial state, making thus the measurements less uncertain.

For an integrated luminosity of 30 fb^{-1}, about 10^5 events are expected which contain a W boson with $p_{\mathrm{T}}^{\mathrm{W}} > 400$ GeV decaying to electron or muon and a neutrino. The expected number for Z production is smaller by an order of magnitude. Given the large statistics and the clean signatures expected for W and Z production, there is a possibility to use these processes for a precise determination (at a level of few percent) of the parton-parton luminosity. Furthermore, the production of gauge boson pairs will provide the opportunity to study electroweak parameters such as the triple gauge boson couplings.

8. HEAVY QUARKS

The production of heavy quarks, due to the quark mass involved, provides an important process for the study of perturbative QCD and of non-perturbative aspects. The total cross section for charm production is 7.8 mb, the one for beauty production is 0.5 mb, while the top-pair produc-

tion cross section is about 0.8 nb.

Due to a large beauty production cross section and a selective trigger, ATLAS can reconstruct large samples of exclusive B-hadron decays [21]. Statistically dominant are the exclusive channels with $J/\psi \to \mu\mu$, which will allow measurements up to $p_T \sim 100$ GeV with negligible statistical errors ($\sim$2000 events with $p_T > 100$ GeV).

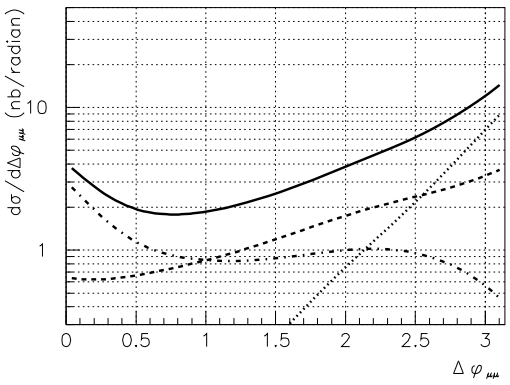

Figure 9. Different mechanisms contributing to azimuthal $\mu\mu$ correlations at the LHC: flavour excitation gb $\to$ gb (dash-dotted line), gluon-gluon fusion gg $\to$ b$\bar{\text{b}}$ (dotted line), gluon-gluon scattering followed by gluon splitting gg $\to$ gg with g $\to$ b$\bar{\text{b}}$ (dashed line), and the sum of all contributions (solid line) [21].

Correlations between b and $\bar{\text{b}}$ quarks, which were difficult to be studied in previous experiments due to limited statistics, will be investigated in detail. In Fig. 9 the expected azimuthal correlation $\Delta\phi_{\mu\mu}$ between the muons from the b and $\bar{\text{b}}$ decays is shown, which provides information on the b–$\bar{\text{b}}$ correlation. The domain of back-to-back kinematics, $\Delta\phi_{\mu\mu} \sim \pi$, is mostly populated by LO QCD contribution. In contrast, the effects of higher orders are more pronounced in the $\Delta\phi_{\mu\mu} \sim 0$ region, which is free of the LO contribution.

Possible deviations from QCD expectations (like new s-channel resonances) should give characteristic signatures in the invariant mass of the t$\bar{\text{t}}$ pair, hence the study of such kinematical distributions is important. Besides that, the extraction of the H/A $\to$ t$\bar{\text{t}}$ decay requires a precise knowledge on the invariant mass distribution, which represents a background process for this channel. Within perturbative QCD the total cross section for top pair production in higher-order corrections is sensitive to the top mass and the scale uncertainty. An error of 1% on the top mass corresponds to an error of 5% in the total t$\bar{\text{t}}$ cross section [1]. Assuming a top quark mass of 175 GeV, the total cross section for t$\bar{\text{t}}$ production is 803 pb at NLO and 833 pb for NLO including the NLL resummation.

9. QUARK COMPOSITENESS

The observation of deviations from QCD predictions of jet rates will reveal new physics such as quark compositeness [22] or the existence of new particles. Measuring the inclusive jet cross section and studying the di-jet mass spectrum and angular distributions are essential tests of QCD.

In the study [23] carried out by ATLAS, the quark substructure, which manifests itself over a compositeness scale Λ, is simulated with PYTHIA [5]. The data simulated in the framework of the Standard Model (SM) are compared with those obtained assuming quark compositeness.

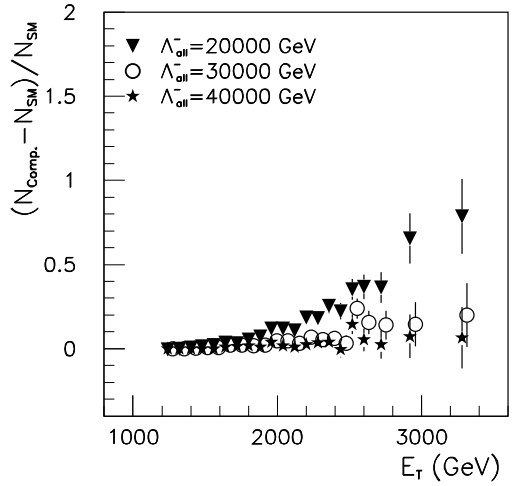

Figure 10. Difference between the SM prediction and the effect of compositeness on the jet E_T distribution, normalized to the SM rate for an integrated luminosity of 300 pb^{-1} [23].

Figure 10 shows the effect of compositeness (all quarks are assumed to be composite) on the inclusive jet energy spectrum, normalized to the SM prediction. The deviation is significant only for large values of E_{T}. However such a signal may be faked either by the uncertainties in the pdf's (equivalent to a signal for $\Lambda = 15$ TeV) or by the non-linear response of the hadron calorimeter. The pdf's are expected to be further constrained before and after LHC starts running (by LHC as well), eliminating thus this background source. If, on the other hand, the calorimeter non-linearity was understood at the 1.5% level, a sensitivity at 95% confidence level (CL) up to Λ equal to 25 (40) TeV for 30 (300) fb^{-1} should be feasible.

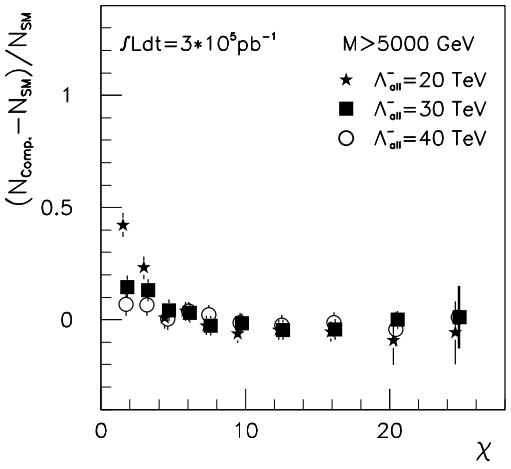

Figure 11. Di-jet angular distribution for di-jet mass above 5000 GeV for an integrated luminosity of 300 pb^{-1} [23].

The angular distribution of the jets is more sensitive to compositeness signals than the jet transverse energy spectrum and less susceptible to calorimeter non-linearities. The analysis is made in terms of the angular variable $\chi \equiv \exp|\eta_1 - \eta_2|$, where $\eta_{1,2}$ are the pseudorapidities of the two leading jets. Figure 11 shows the deviation of the di-jet angular distribution from the SM predictions for invariant di-jet mass larger than 5 TeV. It is clear that quark compositeness leads to an enhancement in the distribution at low values of χ when compared with the SM predictions.

In conclusion, the study demonstrates that the high-mass di-jet angular distribution has an excellent discovery capability for quark compositeness. One month of LHC operation at low luminosity allows discovering quark substructure if the constituent interaction constant is 14 TeV. An integrated luminosity of 300 fb^{-1} is needed to reach a 95% CL limit of 40 TeV.

10. SUMMARY

A variety of QCD-related processes can be studied with the ATLAS detector at the LHC. These measurements are of importance as a study of Quantum Chromodynamics, accessing a new kinematic regime at the highest energy accessible in a laboratory. A precise knowledge and understanding of QCD processes is also essential for the studies of the Higgs boson(s) and searches for new physics beyond the Standard Model, where QCD represents a large part of the background.

Candidate signatures to provide constraints on the quark and anti-quark distributions are the production of W and Z bosons via the Drell-Yan process as well as lepton pair production in general. The production of direct photons, jets, beauty and top quarks can be used to acquire information on the gluon density in the proton.

The precise measurement of the inclusive jet cross section will allow constraints to be set on the strong coupling constant with an uncertainty of $\sim 10\%$. Furthermore, a possible discrepancy between the observed and the theoretically predicted cross section may indicate the discovery of new physics like quark compositeness.

The LHC will extend the kinematic range to larger values of Q^2, the hard scale of the partonic scale, reaching scales of the order of 1 TeV^2. The fraction of the proton momentum attributed to a parton, x, will access values below 10^{-5} with an energy scale above 100 GeV^2.

Acknowledgements

This work has been performed within the ATLAS Collaboration and is the result of collaboration-wide efforts. I would like to thank

the organizers of the *11th International QCD Conference* for the stimulating environment they offered during the event and M. Dobbs for valuable comments on this report. The author acknowledges support by the EU funding under the RTN contract: HPRN-CT-2002-00292, *Probe for New Physics*.

REFERENCES

1. ATLAS Collaboration, *Detector and Physics Performance Technical Design Report* vol. II, CERN/LHCC/99-15, p. 471–543 (1999).[1]
2. W. J. Stirling, "Structure Functions", talk given at the LHCC workshop *Theory of LHC processes*, Feb. 1998, CERN.
3. ATLAS Collaboration, *ATLAS Technical Proposal*, CERN/LHCC/94-43 (1994).[1]
4. A. Moraes, I. Dawson and C. Buttar, "Comparison of predictions for minimum bias event generators and consequences for ATLAS radiation background", ATL-PHYS-2003-020 (2003).[1]
5. T. Sjöstrand, P. Eden, C. Friberg, L. Lonnblad, G. Miu, S. Mrenna and E. Norrbin, Comput. Phys. Commun. **135** (2001) 238 [arXiv:hep-ph/0010017].
6. R. Engel, Z. Phys. C **66** (1995) 203;
   R. Engel, *PHOJET manual (ver. 1.05c, June 1996)*.[2]
7. G. J. Alner *et al.* [UA5 Collaboration], Z. Phys. **33** (1986) 1.
8. F. Abe *et al.* [CDF Collaboration], Phys. Rev. D **41** (1990) 2330.
9. G. Ballistoni and S. Tapprogge, "Studies of hard diffraction in ATLAS", ATL-PHYS-2000-004 (2000).[1]
10. CMS Collaboration, *CMS Technical Proposal*, CERN/LHCC/94-38 (1994).
11. TOTEM Collaboration, Technical Proposal, CERN/LHCC/99-07 (1999).
12. H. Stenzel and S. Tapprogge, "Prospect for QCD jet studies in ATLAS", ATL-PHYS-2000-003 (2000).[1]
13. H. Stenzel, "Determination of α_s using jet cross section parameterizations at hadron collders", ATL-PHYS-2001-003 (2001).[1]
14. M. Wielers, "Isolation of photons", ATL-PHYS-2002-004 (2002).[1]
15. E. M. Abouelouafa and R. Cherkaoui, "On the possibility to determine the gluon structure function in the ATLAS experiment using the direct photon away-side jet cross section at the LHC collider", ATL-PHYS-2001-014 (2001).[1]
16. H. L. Lai *et al.*, Phys. Rev. D **55** (1997) 1280 [arXiv:hep-ph/9606399].
17. A. D. Martin, W. J. Stirling and R. G. Roberts, Phys. Lett. B **354** (1995) 155 [arXiv:hep-ph/9502336].
18. M. Glück, E. Reya and A. Vogt, Z. Phys. C **67** (1995) 433.
19. J. Alitti [UA2 Collaboration], Phys. Lett. B **299** (1993) 174.
20. P. Harriman, A. D. Martin, W. J. Stirling and R. G. Roberts, Phys. Rev. D **42** (1990) 798.
21. S. Baranov and M. Smizanska, "Beauty production overview from Tevatron to LHC", ATL-PHYS-98-133 (1998).[1]
22. E. Eichten, K. D. Lane and M. E. Peskin, Phys. Rev. Lett. **50** (1983) 811;
    E. Eichten, I. Hinchliffe, K. D. Lane and C. Quigg, Rev. Mod. Phys. **56** (1984) 579. [Addendum-ibid. **58** (1986) 1065].
23. Ref. [1], p. 932–939.

[1] All ATLAS documents (TDR, TP, internal notes) are available at the relevant links of the ATLAS web page:
`http://atlas.web.cern.ch/Atlas/internal/Welcome.html`
[2] Available from:
`http://www-ik.fzk.de/~engel/phojet.html`